Acta Crystallographica Section D
Biological Crystallography
ISSN 0907-4449

Structure of mutant human carbonmonoxy-hemoglobin C (βE6K) at 2.0 Å resolution

John C. Dewan,[a] Angela Feeling-Taylor,[c] Yoram A. Puius,[a] Larysa Patskovska,[b] Yury Patskovsky,[a] Ronald L. Nagel,[b,d] Steven C. Almo[a]* and Rhoda Elison Hirsch[b,c]*

[a]Department of Biochemistry, Albert Einstein College of Medicine, Bronx, NY 10461, USA, [b]Department of Medicine (Division of Hematology), Albert Einstein College of Medicine, Bronx, NY 10461, USA, [c]Department of Anatomy and Structural Biology, Albert Einstein College of Medicine, Bronx, NY 10461, USA, and [d]Department of Physiology and Biophysics, Albert Einstein College of Medicine, Bronx, NY 10461, USA

Correspondence e-mail: rhirsch@aecom.yu.edu, almo@aecom.yu.edu

Received 30 May 2002
Accepted 10 September 2002

PDB Reference: HbC(CO), 1k1k, r1k1ksf.

Previous studies have demonstrated that *in vitro* crystallization of R-state liganded hemoglobin C (HbC), a naturally occurring mutant human hemoglobin (βE6K), in high-phosphate buffer solutions provides a potential model system for the intracellular crystallization of HbC associated with chronic hemolytic anemia in CC disease. The first high-resolution crystal structure of liganded HbC is reported here. HbC was crystallized from high phosphate and the structure of the carbonmonoxy-liganded R-state form was refined at 2.0 Å resolution. Crystals exhibit diffraction consistent with the tetragonal space group $P4_12_12$, with unit-cell parameters a = 54.16, c = 195.30 Å. The structure was solved by difference Fourier techniques and refinement by simulated annealing and restrained least-squares yielded a final R of 0.183 and an $R_{\rm free}$ of 0.238 for all 19 382 unique reflections. The side chain of βK6 exhibits very weak electron density consistent with significant mobility within the crystalline lattice. The highly dynamic nature of the side chain could potentially support a number of specific polar interactions that might reduce the barrier to crystallization and thus result in enhanced crystallization kinetics for HbC relative to HbA. Specifically, the NZ atom of the BK6 side chain could participate in an amino–aromatic hydrogen bond with the π-electron cloud of βH116 in a symmetry-related tetramer. βK6 NZ might also interact with the main-chain carbonyl O atom of βH117 and the carboxylate group of βE22 from a symmetry-related tetramer.

1. Introduction

The aggregating β6 mutant human hemoglobins HbC[1] (βE6K) and HbS (βE6V) both give rise to significant pathobiology; however, the mechanistic consequences of the single amino-acid substitutions are dramatically different. Unliganded T-state deoxyHbS forms polymers (Eaton & Hofrichter, 1990; Harrington *et al.*, 1997) within the red blood cells of SS patients (homozygous for HbS), initiating a cascade of pathophysiological events that frequently leads to severe morbidity and mortality in the form of sickle-cell anemia. In contrast, oxy HbC forms intra-erythrocytic crystals. Patients with CC genotype (homozygous for HbC) and SC genotype (heterozygous for HbS and HbC) can exhibit circulating red blood cells containing hemoglobin crystals (Charache *et al.*, 1967; Diggs *et al.*, 1954; Kraus & Diggs, 1956) in the oxygenated liganded state (Hirsch *et al.*, 1985; Lawrence *et al.*, 1991), particularly when splenectomized. Typically, within these cells

[1] HbC, mutant human hemoglobin C (βE6K); HbS, mutant human hemoglobin S (βE6V); HbA, native adult human hemoglobin A; Mb, myoglobin; DPG, 2,3-diphosphoglycerate; r.m.s.d., root-mean-square deviation.

the entire hemoglobin is sequestered into a single crystal, which is surrounded by the plasma membrane. CC patients exhibit a chronic mild hemolytic anemia with little morbidity, in contrast to SC patients that exhibit moderate morbidity and reduced life span [but less than that of SS (sickle cell) patients]. The pathology of SC disease is *not* a consequence of intra-erythrocytic HbC crystal formation, but rather is associated with formation of the deoxyHbS polymers observed in SC erythrocytes (Nagel & Lawrence, 1991; Lawrence *et al.*, 1991). For a review of HbC disorders, see Nagel & Steinberg (2001).

Various red-cell components influence the nucleation kinetics of HbC (Hirsch *et al.*, 1988, 1998; Hirsch, Witkowska *et al.*, 1997; Hirsch, Rybicki *et al.*, 1997; Lin *et al.*, 1989; Nagel *et al.*, 1993) and liganded HbS accelerates HbC nucleation and is incorporated into the liganded HbC crystal (Lin *et al.*, 1988; Patskovska *et al.*, 2000). If HbS could be specifically driven into the HbC crystal, this may have therapeutic significance in reducing the availability of HbS to form polymers in red blood cells of SC patients, since the delay time of HbS aggregation is markedly affected by small changes in hemoglobin concentration or solubility (for a review of HbS delay time, see Eaton & Hofrichter, 1990).

More recently, we have observed that little or no pathology arises in compound heterozygous patients of HbC, including SC compound heterozygotes, that also express hemoglobins shown to increase the nucleation kinetics of liganded HbC crystallization (Nagel *et al.*, 1993; Lawrence *et al.*, 1997). These studies have also served in the identification of some residues involved in the intermolecular contacts of the crystal (Hirsch *et al.*, 1988, 1998; Hirsch, Witkowska *et al.*, 1997; Hirsch, Rybicki *et al.*, 1997; Lin *et al.*, 1989). These contact sites are of significance in the design of therapeutic means to alter rates of nucleation.

Until now, there has been no report of a high-resolution HbC structure (Fitzgerald & Love, 1979). We present here the R-state HbC molecular structure at 2 Å obtained from crystals grown in concentrated potassium phosphate buffer (pH 7.4, 1.75 *M*). This structure has multifold clinical significance that will help further the understanding of molecular mechanisms involved in the aforementioned hemoglobinopathies and in the recently reported protective effect of the CC genotype against life-threatening human malaria induced by *Plasmodium falciparum* (Modiano *et al.*, 2001).

2. Experimental

2.1. Protein purification and crystallization

CC human blood was obtained from individuals according to clinical protocols approved by the Albert Einstein College of Medicine. $HbC(O_2)$ was purified from red blood cell hemolysates *via* CM-52 cation-exchange chromatography employing gradient elution from 10 m*M* sodium phosphate pH 6.8 to 50 m*M* sodium phosphate pH 8.4. Samples were characterized by cellulose acetate gel electrophoresis and concentrated to greater than 120 mg ml^{-1}. Solutions of $HbC(O_2)$ were converted to HbC(CO) by exposure to CO gas without bubbling. Complete conversion and the absence of metHbC were confirmed by the examination of visible spectra at 500–700 nm. HbC(CO) was chosen for study rather than $HbC(O_2)$ because (i) hemoglobin is more stable in the CO form, being less prone to oxidation (Baldwin, 1980; Shaanan, 1983), (ii) only minor differences exist between the crystal structures of R-state HbA(CO) and $HbA(O_2)$ (Shaanan, 1983) and (iii) crystal morphology and nucleation kinetics are essentially identical for HbC(CO) and $HbC(O_2)$ (Hirsch *et al.*, 1988).

Table 1
Data-collection and refinement statistics.

Diffraction data	
Space group	$P4_12_12$
Resolution range (Å)	2.00–22.50
Completeness (%)	94.00
R_{merge} (I)	0.063
No. of reflections	
Total	84880
Unique	19382
Structure refinement	
R_{cryst} (%)	18.30
R_{free} (%)	23.80
No. of protein atoms	2192
No. of heteroatoms	90
No. of solvent atoms	113
Average B factor (Å^2)	
Protein	24.9
Solvent	51.3
R.m.s. deviations from ideal	
Bonds (Å)	0.007
Angles (°)	1.12

Crystals were grown at ambient temperature by a modification of the batch method (Hirsch *et al.*, 1988) using HbC(CO) at a final concentration of 20 mg ml^{-1} and a range of potassium phosphate concentrations (1.5–1.8 *M*, pH 7.35). Mixtures were exposed to CO gas, without bubbling, 3–4 times per week. Large crystals (∼1 mm) grew within 3–10 d from a batch having a phosphate concentration of 1.75 *M*. Diffraction from these crystals is consistent with the tetragonal space group $P4_12_12$, with unit-cell parameters $a = 54.16$, $c = 195.30$ Å. The asymmetric unit consists of one $\alpha\beta$ dimer, giving four $(\alpha\beta)_2$ hemoglobin tetramers per unit cell. The dimer in the asymmetric unit is designated $\alpha_1\beta_1$, while the $\alpha_2\beta_2$ dimer generated by the crystallographic symmetry operation $(-y+1, -x+1, \frac{1}{2}-z)$ completes the tetramer.

2.2. Data collection and processing

X-ray data to 2.0 Å were collected at room temperature using Cu $K\alpha$ radiation ($\lambda = 1.5418$ Å) with a Siemens X-1000 multiwire area detector coupled to a Rigaku RU-200 rotating-anode generator. Data were reduced and scaled with *XDS* and *XSCALE* (Kabsch, 1988), respectively, resulting in a merging R factor of 6.3% and 94% overall completeness (Table 1).

2.3. Structure refinement

The 1hho structure, which is isomorphous and essentially isostructural with HbC(CO) (Fig. 1), was used to initiate

refinement. The CO ligands were excluded from the initial model and the mutant βK6 residue was included as Ala. Several rounds of refinement using data in the 22.5–2.0 Å resolution range and consisting of simulated-annealing, positional and individual isotropic *B*-factor refinements were performed with *X-PLOR* (Brünger, 1996). A test set of reflections, consisting of 9.8% of the data, was used throughout the refinement for the determination of $R_{\rm free}$ (Brünger, 1992*a*,*b*). Each round of refinement was followed by manual rebuilding of the model with *TOM* (Jones, 1985; Jones & Thornton, 1996). Side chains of disordered residues were replaced by Ala and fit into $2F_o - F_c$ difference Fourier maps, followed by further refinement.

Water molecules were located in $2F_o - F_c$ maps as peaks with electron density greater than 1.0σ that were within 2.5–3.5 Å of a hydrogen-bond donor or acceptor, gave acceptable hydrogen-bond geometry and did not appear to be part of a disordered side chain. At later stages in the refinement, only positional and *B*-factor refinements were performed. In all but the final cycle of refinement, water molecules were deleted from the model if their *B* factor exceeded 90 Å^2. The CO ligands were also included at this stage and an isotropic bulk-solvent correction was applied (Jiang & Brünger, 1994). The side chain of βK6 was only represented by weak electron density and could only be modeled into continuous density at the 0.5σ level in a $2F_o - F_c$ map, which exhibited considerable noise. Thus, this residue must be considered highly dynamic.

The final model consists of 2192 non-H protein atoms from the 141-residue α-chain, the 146-residue β-chain, the 90 atoms of two CO-liganded heme groups and 113 water molecules, with *R* and $R_{\rm free}$ of 0.183 and 0.238, respectively. The average *B* factor for all protein atoms is 24.9 Å^2, while the average *B* factor for water molecules is 51.3 Å^2. The model displays excellent stereochemistry, with r.m.s.d. bond lengths and angles of 0.007 Å and 1.12°, respectively. No residues were modeled with alternative side-chain conformations and all occupied allowed regions of the Ramachandran plot. The programs *PROCHECK* (Laskowski *et al.*, 1993) and *WHAT_CHECK* (Vriend & Sander, 1993) were used to verify the stereochemical quality of the final model. The quality of the electron-density map (*e.g.* at the heme site) is illustrated (Fig. 2).

3. Results and discussion

3.1. HbC(CO) adopts the R-state quaternary structure

The present structure of HbC(CO) clearly demonstrates that it adopts the R state and demonstrates that minor differences in pH and phosphate concentration appear to have little effect on the hemoglobin molecule, as all R-state hemoglobin structures are very similar. The structures with which HbC(CO) are best compared are 1aj9 and 1hho. The 1aj9 structure determination was undertaken to update the 2hco PDB entry, but refinement revealed that the determination had actually been performed on the naturally occurring human αA53S mutant. This mutation on the surface

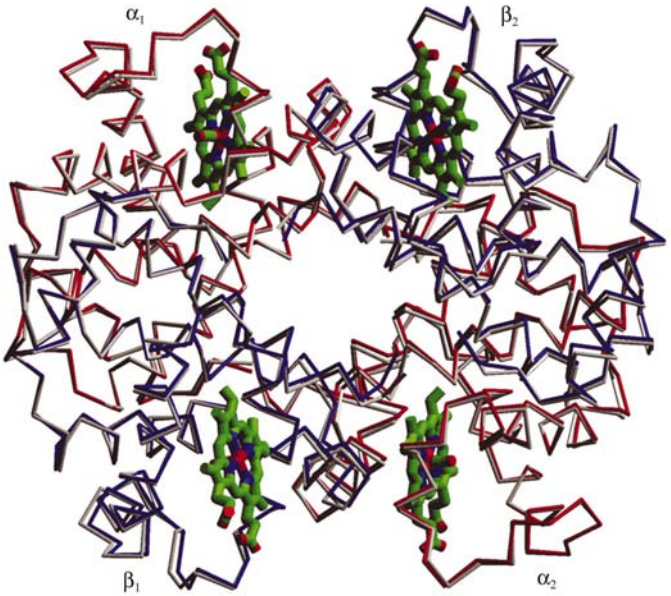

Figure 1
Superposition of COHbC (PDB code 1k1k) and the R-state oxyHbA (PDB code 1hho) quaternary structures (only C^{α} backbone atoms are shown) show that COHbC and oxyHbA are isomorphous and essentially isostructural. The model for HbA is colored grey. α- and β-subunits of COHbC are presented in red and blue respectively. Hemes are drawn as stick models with carbon atoms shown in green. Both hemoglobin tetramers were generated from $\alpha\beta$ heterodimers using crystallographic symmetry operators.

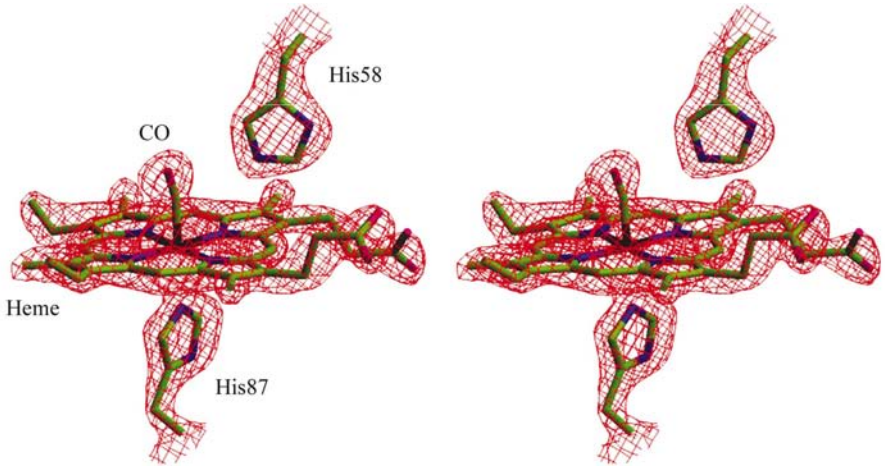

Figure 2
Electron-density map of the α-chain heme pocket of the 2Δ resolution of COHbC showing the high quality of the electron-density map, as exemplified by the proximal and distal histidines, and the heme group and CO molecule. Stereoview of $2F_o - F_c$ electron-density contour map built around the heme, His58 and His87 of the α-subunit of COHbC.

of the tetramer reportedly causes no observable perturbation to the molecule (Vásquez *et al.*, 1998).

The significant similarity amongst the HbC(CO), 1aj9 and 1hho structures is evident from a superposition of equivalent C^{α} atoms carried out using *ProFit* (Martin, 1995). The r.m.s.d. between the α-chains of HbC(CO) and 1aj9 is 0.28 Å, between HbC(CO) and 1hho is 0.30 Å and between 1aj9 and 1hho is 0.38 Å. For the β-chains these values are 0.31, 0.38 and 0.42 Å, respectively, and for the complete $\alpha\beta$ dimer the values are 0.30, 0.36 and 0.41 Å, respectively. Difference distance matrix plots produced with *DDMP* (Center for Structural Biology, Yale University, New Haven, CT, USA) further highlight the structural similarity between these structures. When the α- and β-chains are considered independently, they reveal that the majority of differences, none of which exceeds 1.9 Å, involve residues α1, α141 and β146 at the N- and C-termini. This is also the case when the $\alpha\beta$ dimers are considered as a unit. Terminal residues of all *R*-state structures suffer disorder (Perutz, 1970, 1976, 1990; Baldwin & Chothia, 1979; Baldwin, 1980; Shaanan, 1983) and the observed structural differences are likely to reflect the difficulty and subjectivity in placing them in the weak electron density. This disorder may be relevant as the rupture of the intersubunit hydrogen bonds at the α- and β-chain C-termini upon undergoing the T–R transition is central to the Perutz (1970, 1976, 1990) mechanism of hemoglobin cooperativity.

The largest C^{α} differences, other than those involving chain termini, occur at residue βA76, with a 1.53 Å C^{α}-atom difference being observed between HbC(CO) and 1hho and a 1.42 Å difference between 1aj9 and 1hho. The deviations arise from a conformational difference in the βG74–βH77 turn of the *EF* loop region in 1hho when compared with the same region in HbC(CO) and 1aj9 and has been noted previously by Vásquez *et al.* (1998). The C^{α} difference between HbC(CO) and 1aj9 at βA76 is 0.40 Å. The small r.m.s.d. values for the superposition of equivalent C^{α} positions of HbC(CO), 1aj9 and 1hho and the similarity of the C^{α} difference distance matrices attest to the lack of perturbation by surface alterations in these structures.

3.2. Phosphate-binding sites

No phosphate anions have been assigned in HbC(CO). In 1hho there is a single phosphate positioned on a crystallographic twofold axis and the same site is observed in the αV96W mutant (PDB code 1rvw; Puius *et al.*, 1998). The site lies in the central cavity of the tetramer, close to the DPG-binding site of the T-state structure (Arnone, 1972; Richard *et al.*, 1993) and differs from the phosphate-binding site assigned in the asymmetric unit of 1aj9 at the $\alpha_1\beta_2$ interface. In HbC(CO), there are no water molecules at the position equivalent to the 1hho phosphate-binding site, although a single water molecule is located 0.7 Å from the site observed in 1aj9. However, as its refined *B* factor of 54.3 $Å^2$ is close to the average of 51.3 $Å^2$ observed for all HbC(CO) water molecules, it is unlikely to represent a phosphate site.

3.3. The βE6K mutation site

The increased propensity of R-state HbC to crystallize more readily *in vitro* is presumably the consequence of unique inter-tetrameric interactions that are not available to HbA. Replicas of freeze-etched intra-erythrocytic crystals revealed subunit particles measuring about 65 × 100 Å arrayed in a non-cubic monoclinic pattern resembling either a tetragonal or hexagonal arrangement, depending on the region of the crystal viewed (Lessin *et al.*, 1969). Atomic force microscopy has demonstrated that this array appears similar to that observed in R-state (CO) HbC crystals grown under the same conditions used for the present structure determination (Feeling-Taylor, 2002; Vekilov *et al.*, 2003).

The βK6 mutation site resides in the *A* helix on the surface of the β-chain. In these crystals, the side chain of this residue appears to be highly mobile, as evidenced by very weak electron density. Modeling suggests that βK6 ε-amino group (NZ) could participate in several potential interactions, including an amino–aromatic interaction with the π-electron cloud of the imidazole ring of βH116 in a symmetry-related tetramer. A similar interaction was observed in hen ovotransferrin involving Lys and Tyr residues (Dewan *et al.*, 1993) and Vásquez *et al.* (1998) suggested similar interactions in 1aj9 involving two His residues. Additional interactions available to the βK6 side chain on the basis of distance considerations are potential hydrogen bonds between βK6 NZ and βH117 O and between the positively charged βK6 NZ and the negatively charged carboxylate group of βE22. Another possible interaction is that involving βK6 NZ and the π-electron cloud of βH117. The absence of highly populated polar interactions involving βK6 NZ may be the consequence of the very high ionic strength used for crystallization. Alternatively, some subset of these polar interactions, in particular the potential salt bridge between βK6 NZ and βE22, may only form transiently during the transition state for nucleation and do not contribute to the ground-state stability of the crystalline lattice.

4. Conclusion

The present structure (PDB code 1k1k) demonstrates that HbC(CO) crystals grown from high concentrations of phosphate, exhibit the R-state quaternary conformation similar to HbA(oxy) (PDB code 1hho). The HbC(CO) structure also highlights the extensive mobility of βK6 and suggests potential ionic interactions that are responsible for driving the intra-erythrocytic crystal formation associated with CC and SC diseases in humans.

This research is supported in part by the American Heart Association, Heritage Affiliate grants-in-aid 9950989T and 9950989T (REH), the National Institutes of Health Biomedical Technology Program P41-RR01633 (SCA), the National Institutes of Health NHLBI R01-HL58038 (REH), P01-HL55435 (RLN), P60-HL38655 (RLN) and 1F31-HL09564 (AFT), and Universities Space Research Associa-

tion Research Contract 03537.000.013 (REH). YAP and AF were students in the Medical Scientist Training Program of the Albert Einstein College of Medicine (NIH T32-GM07288).

References

Arnone, A. (1972). *Nature (London)*, **237**, 146–149.
Baldwin, J. & Chothia, C. (1979). *J. Mol. Biol.* **129**, 175–220.
Baldwin, J. M. (1980). *J. Mol. Biol.* **136**, 103–128.
Brünger, A. T. (1992*a*). *Nature (London)*, **355**, 471–475.
Brünger, A. T. (1992*b*). *X-PLOR Version* 3.1. *A System for X-ray Crystallography and NMR.* Yale University, New Haven, CT, USA.
Brünger, A. T. (1996). *X-PLOR Version* 3.851. *A System for X-ray Crystallography and NMR.* Yale University, New Haven, CT, USA.
Charache, S., Conley, C. L., Waugh, D. F., Ugoretz, R. J. & Spurrell, J. R. (1967). *J. Clin. Invest.* **46**, 1795–1811.
Dewan, J. C., Mikami, B., Hirose, M. & Sacchettini, J. C. (1993). *Biochemistry*, **32**, 11963–11968.
Diggs, L. W., Kraus, A. P., Morrison, D. B. & Rudnicki, R. P. T. (1954). *Blood*, **9**, 1172–1184.
Eaton, W. A. & Hofrichter, J. (1990). *Adv. Protein Chem.* **40**, 63–279.
Feeling-Taylor, A. (2002). Doctoral dissertation, Albert Einstein College of Medicine, Bronx, NY, USA.
Fitzgerald, P. M. D. & Love, W. E. (1979). *J. Mol. Biol.* **132**, 603–619.
Harrington, D. J., Adachi, K. & Royer, W. E. (1997). *J. Mol. Biol.* **272**, 398–407.
Hirsch, R. E., Lin, M. J. & Nagel, R. L. (1988). *J. Biol. Chem.* **263**, 5936–5939.
Hirsch, R. E., Raventos-Suarez, C., Olson, J. A. & Nagel, R. L. (1985). *Blood*, **66**, 775–777.
Hirsch, R. E., Rybicki, A. C., Fataliev, N. A., Lin, M. J., Friedman, J. M. & Nagel, R. L. (1997). *Br. J. Haematol.* **98**, 583–588.
Hirsch, R. E., Shafer, F., Wajcman, H., Fataliev, N. & Nagel, R. L. (1998). *Blood*, **92**(*Suppl.*), 11a.
Hirsch, R. E., Witkowska, H. E., Shafer, F., Lin, M. J., Balazs, T. C., Bookchin, R. M. & Nagel, R. L. (1997). *Br. J. Haematol.* **97**, 259–265.
Jiang, J.-S. & Brünger, A. T. (1994). *J. Mol. Biol.* **243**, 100–115.
Jones, T. A. (1985). *Methods Enzymol.* **115**, 157–171.
Jones, S. & Thornton, J. M. (1996). *Proc. Natl Acad. Sci. USA*, **93**, 13–20.
Kabsch, W. (1988). *J. Appl. Cryst.* **21**, 916–924.
Kraus, A. P. & Diggs, L. W. (1956). *J. Lab. Clin. Med.* **47**, 700–705.
Laskowski, R. A., MacArthur, M. W., Moss, D. S. & Thornton, J. M. (1993). *J. Appl. Cryst.* **26**, 283–291.
Lawrence, C., Fabry, M. E. & Nagel, R. L. (1991). *Blood*, **78**, 2104–2112.
Lawrence, C., Hirsch, R. E., Fataliev, N. A., Patel, S., Fabry, M. E. & Nagel, R. L. (1997). *Blood*, **90**, 2819–2825.
Lessin, L. S., Jensen, W. N. & Ponder, E. (1969). *J. Exp. Med.* **130**, 443–466.
Lin, M. J., Nagel, R. L. & Hirsch, R. E. (1989). *Blood*, **74**, 1823–1825.
Martin, A. C. R. (1995). *ProFit V1.6: Protein Least Squares Fitting.* SciTech Software, Ashtead, Surrey, England.
Modiano, D., Luoni, G., Sirima, B. S., Simpore, J., Verra, F., Konate, A., Rastrell, E., Oliveri, A., Calissano, C., Pananotti, G. M., D'Urbano, L., Sanou, I., Sawadogo, A., Modiano, G. & Coluzzi, M. (2001). *Nature (London)*, **414**, 305–308.
Nagel, R. L. & Lawrence, C. (1991). *Hematol. Oncol. Clin. North Am.* **5**, 433–51.
Nagel, R. L., Lin, M. J., Witkowska, H. E., Fabry, M. E., Bestak, M. & Hirsch, R. E. (1993). *Blood*, **82**, 1907–1912.
Nagel, R. L. & Steinberg, M. H. (2001). *Disorders of Hemoglobin: Genetics, Pathophysiology and Clinical Management*, edited by M. H. Steinberg, B. G. Forget, D. R. Higgs & R. L. Nagel, pp. 756–785. Cambridge University Press.
Patskovska, L., Patskovsky, Y., Nagel, R. L., Almo, S. C. & Hirsch, R. E. (2000). *Annual Sickle Cell Meeting Program.* Manuscript in preparation.
Perutz, M. F. (1970). *Nature (London)*, **228**, 726–739.
Perutz, M. F. (1976). *Br. Med. Bull.* **32**, 195–208.
Perutz, M. F. (1990). *Annu. Rev. Physiol.* **52**, 1–25.
Puius, Y. A., Zou, M., Ho, N. T., Ho, C. & Almo, S. C. (1998). *Biochemistry*, **37**, 9258–9265.
Richard, V., Dodson, G. G. & Mauguen, Y. (1993). *J. Mol. Biol.* **233**, 270–274.
Shaanan, B. (1983). *J. Mol. Biol.* **171**, 31–59.
Vásquez, G. B., Ji, X., Fronticelli, C. & Gilliland, G. L. (1998). *Acta Cryst.* D**54**, 355–366.
Vekilov, P. G., Feeling-Taylor, A. & Hirsch, R. E. (2003). In *Methods in Molecular Medicine*, Vol. 82, *Hemoglobin Disorders, Molecular Methods and Protocols*, edited by R. L. Nagel. New Jersey: Humana Press. In the press.
Vriend, G. A. & Sander, C. (1993). *J. Appl. Cryst.* **26**, 47–60.